

RESEARCH PAPER

Effects of Crystalline Form on the Tableting Compression Mechanism of Phenobarbital Polymorphs

M. Otsuka,* M. Nakanishi, and Y. Matsuda

Department of Pharmaceutical Technology, Kobe Pharmaceutical University, Motoyama-Kitamachi 4-19-1, Higashi-Nada, Kobe 658, Japan

ABSTRACT

The effects of the polymorphic form on the compression mechanism of forms A, B, and F of phenobarbital were investigated using a compression simulator, mercury porosimetry, X-ray diffraction analysis, BET gas absorption method, and scanning electron microscopic (SEM) photography. The order of tablet hardness obtained from all phenobarbital polymorphs was form A > form B > form F in accordance with that of the specific surface area. The Cooper and Eaton method was applied to evaluate two individual compression processes: particle rearrangement (phase I) and fragmentation and/or deformation (phase II). The parameters for compression processes were calculated using a nonlinear regression analyses program, and the compression energies of phases I and II were calculated from these parameters. The relationship between specific surface area after compression and compression energy at phase I showed a good linear correlation, but their ratio did not. In contrast, the specific surface area ratio showed a linear relationship with the compression energy on phase II, but again the ratio of these two parameters did not. The tablet hardness showed a linear relationship with the specific surface area ratio, but not with the specific surface area. Again, the ratio of these two parameters did not show a linear relationship.

* To whom correspondence should be addressed.

INTRODUCTION

Changes in the physicochemical properties of bulk and excipient powders such as particle size, crystal habit, specific surface, powder flowability, and the like will often be induced during preparation (drying, recrystallization, spray drying, grinding and compression), and these properties affect tablet hardness, tablet lamination, disintegration time and dissolution rate of the preparations reflecting the dynamic tableting behavior (1,2). There have been many investigations with regard to tableting or compression as preformation studies (3–15). However, the effects of the polymorphic crystalline form on tableting behavior and tablet properties have not been completely elucidated.

Previously, we investigated the effects of temperature on the polymorphic transformation and dynamic tableting characteristics (16) of chlorpropamide polymorphs using the Cooper and Eaton analysis (17) and Heckel analysis (18,19) and concluded that the tableting characteristics of the crystalline powders were affected by tableting temperature and the powders' polymorphic form.

Phenobarbital is widely used as a hypnotic or sedative drug, and there have been many reports concerning polymorphic modifications (20–24), dissolution rates (25), bioavailability (26), stability (27), and tablet hardness (28) of this drug. However, there have been no reports concerning the tableting properties of phenobarbital.

In this study, therefore, we investigated the dynamic tableting characteristics of phenobarbital polymorphic forms to evaluate their pharmaceutical properties.

MATERIALS AND METHODS

Materials

Bulk phenobarbital powder of JP grade (lot T46513) was obtained from Maruishi Pharmaceutical Company, Osaka, Japan. Three kinds of phenobarbital modifications, forms A, B, and F, were prepared by previously reported (11) methods. The sample powders of all polymorphic forms with average particle diameter 49.5 μm were obtained by sieving with 37- μm and 62- μm screens.

Micrometric Characterization

The true densities of the powders were determined using an air comparison pycnometer (model 930; Beckman-Toshiba Co., Tokyo, Japan). The specific surface area S_w was measured with a gas adsorption apparatus (one-point method; Flow sorb, model 2300, Shimadzu Co., Kyoto,

Japan) using BET gas adsorption. The adsorption gas used for measurement contained 30% N_2 and 70% He. All values represent averages of four measurements.

X-Ray Powder Diffraction Analysis

Diffractionograms were taken at room temperature with an X-ray diffractometer (XD-3A, Shimadzu Co., Kyoto, Japan). The operating conditions were as follows: target, copper; filter, nickel; voltage, 25 kV; current, 10 mA; receiving slit, 0.1 mm; time constant, 1 sec; counting range, 1 kcps; scanning speed 4° 2 θ /min.

Tableting Apparatus and Procedures

A compression/tension tester (Autograph, model IS-5000, Shimadzu Co., Kyoto, Japan) with two load cells (upper and lower punches) and a displacement transducer was used to measure the upper and lower compression force and displacement at 25°C \pm 1°C. Samples of 200 mg were compressed by an 8-mm die and punches with a flat surface at 49, 98, and 196 MPa (maximum upper-punch pressure) at a compression speed of 15 mm/min.

Calculation of Compression Energy

Density functions were used for Cooper and Eaton analysis (17) as described below. The computer program MULTI (29) was used for the nonlinear least-squares fit of the compression profiles shown in Eq. 1. The compression parameters were calculated using the damping Gauss-Newton method after the initial values of the parameters were determined by the Simplex method. A weight of unity was used in this analysis. The values were the means \pm SD of three replicates. Compression energies of phases I and II were estimated from the simulated curves based on Eq. 1.

Statistical Analysis

Student's *t* test was used to determine the significance of differences and a *p* value of .05 was considered significant.

Tablet Hardness

The hardness of the tablets was measured three times using a hardness tester (Toyama Co.).

Micropore Distribution

The micropore distribution of the tablets was measured by mercury porosimetry (Porosimeter 2000, Carlo Erba Instruments, Japan). The pore size ranged from 50 to 6×10^{-3} μm .

RESULTS

Physicochemical Characterization of Phenobarbital Modifications

Figure 1 shows the powder X-ray diffraction profiles of three polymorphic forms of phenobarbital before and after compression at 196 MPa. All forms had characteristic diffraction peaks, as reported previously (27). Form A had diffraction peaks at 17.1° , 21.1° , and 28.6° ; those for form B were at 7.4° , 14.1° , 17.3° , and 22.5° ; and those for form F were at 7.4° , 15.8° , and 22.5° (20). After compression at 196 MPa, their diffraction patterns did not change except for decreases in intensity at a low diffraction angle. Table 1 shows the results of micrometric characterization of the polymorphic forms of phenobarbital. Form A had the largest specific surface area and the lowest apparent specific volume. These results suggested that forms A, B, and F had specific powder characteristics.

Dynamic Compression Process of Phenobarbital Polymorphs

Figure 2 shows the dynamic compression process of phenobarbital polymorphic forms. The compression pro-

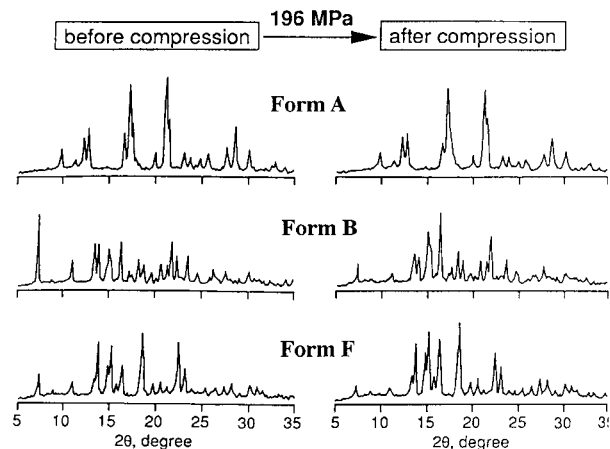


Figure 1. Powder X-ray diffraction profiles of three polymorphic forms of phenobarbital.

files of form B were almost the same as that of form F, but the powder bed thickness of form A was much larger than those of forms B and F.

Pharmaceutical materials are normally consolidated by movement and rearrangement of initial particles, followed by fragmentation and elastic or plastic deformation of smaller particles. First, we evaluated phases I and II using a Cooper plot (17). This analysis was based on dividing the compression processes into two stages, particle rearrangement and fragmentation and/or deformation, according to Eq. 1.

$$\frac{V_0 - V}{V_0 - V_i} = a_1 \exp \left\{ -\frac{k_1}{P} \right\} + a_2 \exp \left\{ -\frac{k_2}{P} \right\} \quad (1)$$

where V_0 is the volume of the powder at zero pressure, V is volume of the tablet at pressure P , V_i is the true volume of the solid present in the tablet, a_1 is the fraction of theoretical compaction that would be achieved at infinite pressure for the filling of voids of the same dimensions as the particles by rearrangement, a_2 is the fraction of theoretical compaction that would be achieved at infinite pressure for the filling of voids smaller than the particles by fragmentation and/or deformation, and k_1 and k_2 are coefficients with units of pressure that indicate the magnitude of the pressure at which the particular process has the greatest probability density.

Phase I in Eq. 1 is the filling of holes of the same dimensions as the particles by rearrangement, while phase II is the filling of holes smaller than the particles by fragmentation and plastic flow. This method is thought to be useful for evaluating nonfragmented materials.

Figure 3 shows the Cooper plot of the compression process of form A at 196 MPa. The parameters for compression processes of all polymorphic forms were calculated from the Cooper plots using nonlinear regression analyses software (29) and are summarized in Table 2. The theoretical values (shown by the solid lines in the figure) were in good agreement with the observed values under all compression conditions and the phase I (Δ) and II (\blacklozenge) compression processes obtained by the calculation based on the compression parameters.

Figure 4 shows the phase I and II compression processes of all polymorphic forms at 196 MPa obtained by the simulation method and the compression energies of phases I and II estimated from the simulation curves. The compression process of form A resisted more during the phase I process than those of forms B and F, which means the friction from A powder with the die wall and/or between particles in the powder bed was larger than that of forms B and F. In contrast, the phase II compression pro-

Table 1

Micrometric Characterization of Polymorphic Forms of Phenobarbital

Sample	δ_i (g/cm ³)	V_a (cm ³ /g)	S_w (m ² /g)	d (μ m)
A form	1.324 \pm 0.012	2.20 \pm 0.08	2.34 \pm 0.11	49.5
B form	1.391 \pm 0.015	2.34 \pm 0.06	0.432 \pm 0.016	49.5
F form	1.368 \pm 0.013	2.29 \pm 0.09	0.441 \pm 0.015	49.5

δ_i , true powder density; v_a , apparent specific volume; S_w , specific surface area ($n = 3$); d , the sample powders were prepared and sieved to a fraction of 37–62 μ m.

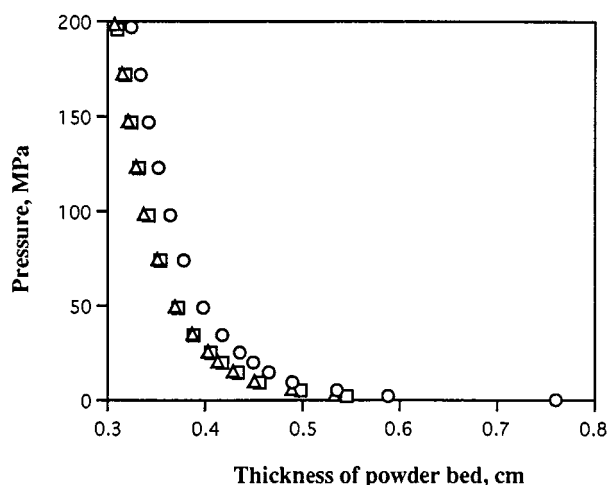


Figure 2. The dynamic compression process of phenobarbital polymorphic forms at 196 MPa: \circ , form A; \triangle , form B; \square , form F.

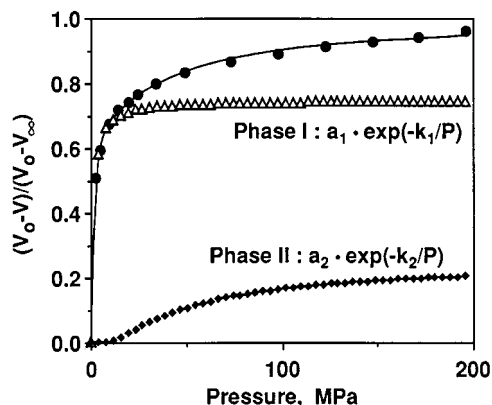


Figure 3. Cooper plot of the compression process of form A at 196 MPa.

cess of form A progressed further than those of the other forms.

The a_1 values of all forms of phenobarbital polymorphs increased with increasing compression pressure, but the a_2 values decreased. The $a_1 + a_2$ values of all compression processes increased with increasing pressure and approached 1; and the value of form A at 49 MPa (0.899) was the lowest obtained. The k_1 and k_2 values of form A were larger than those of forms B and F at each compression pressure tested.

Figure 5 shows the relationship between compression energies of phases I and II and maximum compression stress of polymorphic forms. Compression energy at phase II was about 4 to 5 times larger than that at phase I, and those of all samples increased with increasing maximum compression stress. Compression energy at phase I of form A was larger than for the other forms, and the order was form A > form F > form B, indicating that particle rearrangement of form A powder required more energy than the other samples.

On the other hand, the compression energy at phase II of form A was almost the same as for the other forms at lower pressure, except for that of form A at 196 MPa, indicating that the hardnesses of all crystals were not much different between the polymorphic forms.

Physical Characterization of Tablets Obtained from Phenobarbital Polymorphic Forms

Tables 3 and 4 show the results of micrometric characterization of the powders and tablets obtained from various polymorphic forms of phenobarbital. The order of tablet tensile strength obtained from all phenobarbital polymorphs was form A > form B > form F in accordance with that of the specific surface area. However, the order of thickness of ejected tablets was form A > form F > form B.

Table 2
Compression Parameters Calculated from Cooper's Equation

Form	Pressure (MPa)	Parameters				
		a_1	a_2	$a_1 + a_2$	k_1 (MPa)	k_2 (MPa)
A	49	0.552 ± 0.002	0.337 ± 0.001	0.889	0.305 ± 0.009	7.25 ± 0.171
	98	0.654 ± 0.009	0.285 ± 0.006	0.939	0.530 ± 0.044	15.9 ± 0.715
	196	0.747 ± 0.005	0.254 ± 0.006	1.001	0.973 ± 0.034	44.1 ± 0.950
B	49	0.631 ± 0.002	0.283 ± 0.002	0.914	0.084 ± 0.005	6.73 ± 0.134
	98	0.712 ± 0.003	0.245 ± 0.003	0.957	0.222 ± 0.005	14.4 ± 0.346
	196	0.793 ± 0.004	0.202 ± 0.003	0.995	0.606 ± 0.047	38.7 ± 1.734
F	49	0.605 ± 0.003	0.316 ± 0.004	0.921	0.110 ± 0.005	6.60 ± 0.045
	98	0.685 ± 0.002	0.272 ± 0.001	0.957	0.267 ± 0.002	12.4 ± 0.281
	196	0.789 ± 0.004	0.209 ± 0.003	0.998	0.739 ± 0.023	37.0 ± 0.929

Values represent means \pm SD of three experiments.

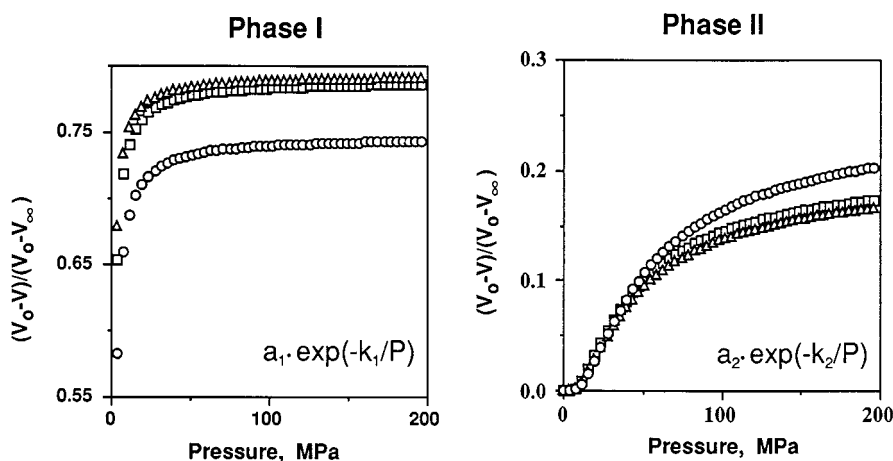


Figure 4. Phases I and II of the compression processes of all polymorphic forms at 196 MPa obtained by the simulation method: ○, form A; △, form B; □, form F.

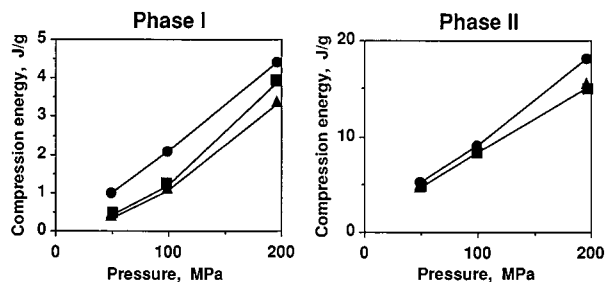


Figure 5. The relationship between compression energies of phases I and II and maximum compression stress of polymorphic forms: ●, form A; ▲, form B; ■, form F.

Figure 6 shows the pore distribution of tablets obtained from polymorphic forms of phenobarbital. The pores of about 100 μm of form A were larger than those of the other forms, but the order of total pore volume was form F > form B > form A.

Figure 7 shows scanning electron microscopy (SEM) photographs of the samples before and after compression. Form A was comprised of plate particles 80–100 μm in length, 50 μm width, and 20–40 μm thick with micropores of less than 2 μm in diameter. Form B consisted of plate crystals with smooth surfaces, and the particles were about 100 μm in length, 50 μm in width, and 20–40 μm in thickness. Form F was comprised of plate crystals with smooth surfaces, and the particles were 100–

Table 3

Micrometric Characterization of Tablets Obtained from Various Polymorphic Forms of Phenobarbital

Sample	TS (kg/cm ²)	L_t (cm)	L_c (cm)	E	ρ (mm ³ /g)
A form	22.0 ± 1.6	0.3394 ± 0.005	0.3231 ± 0.005	1.050	118.2
B form	11.2 ± 2.2	0.3237 ± 0.001	0.3082 ± 0.006	1.050	88.5
F form	8.2 ± 0.7	0.3302 ± 0.001	0.3101 ± 0.003	1.065	123.6

Tablets were obtained by compression at 196 MPa. TS, tensile strength; L_t , thickness of the tablet after ejection; L_c , thickness of the powder bed under compression; E , Young's modulus of tablet (L_t/L_c); ρ , cumulative pore volume in the tablet after compression ($n = 3$).

Table 4

Specific Surface Area and Hardness of Tablets Obtained from Polymorphic Forms of Phenobarbital

Sample	TH (kg/cm ²)	S_w (m ² /g)	S_{wp} (m ² /g)	S_{wp}/S_w
A form	22.0 ± 1.6	2.34 ± 0.11	1.91 ± 0.04	0.816
B form	11.1 ± 2.2	0.432 ± 0.011	1.19 ± 0.02	2.75
F form	8.2 ± 0.7	0.441 ± 0.015	1.53 ± 0.03	3.47

Tablets were obtained by compression at 196 MPa. TH, tablet hardness; S_{wp} , specific surface area after compression ($n = 3$).

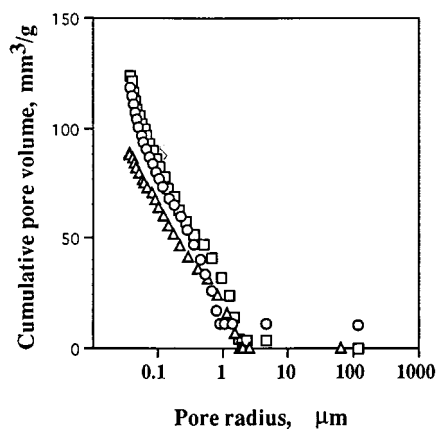


Figure 6. Pore distributions of the tablets obtained from polymorphic forms of phenobarbital: ○, form A; △, form B; □, form F.

150 μm in length, 50 μm in width, and 20–40 μm thick. After compression at 196 MPa, the tablet surface of form A was relatively flat and consisted of very fine particles, but the surfaces of forms B and F were irregular and comprised of particles that ranged in size from less than 5 μm to 50 μm in diameter.

Relation Between Physical Properties of Tablets Obtained from Phenobarbital Polymorphic Forms and Their Compression Parameters

Figure 8 shows the relationship between the void space of tablets and/or their ratio and the compression energies with regard to phases I and II. The void space ratio and void space after compression at 196 MPa increased with increasing compression energy in phase I, but those of phase II did not.

Figure 9 shows the relationship between specific surface area of tablets and/or their ratio and compression energies with regard to phases I and II. The specific surface area and compression energy showed a good linear relationship at phase I, but their ratio did not. In contrast,

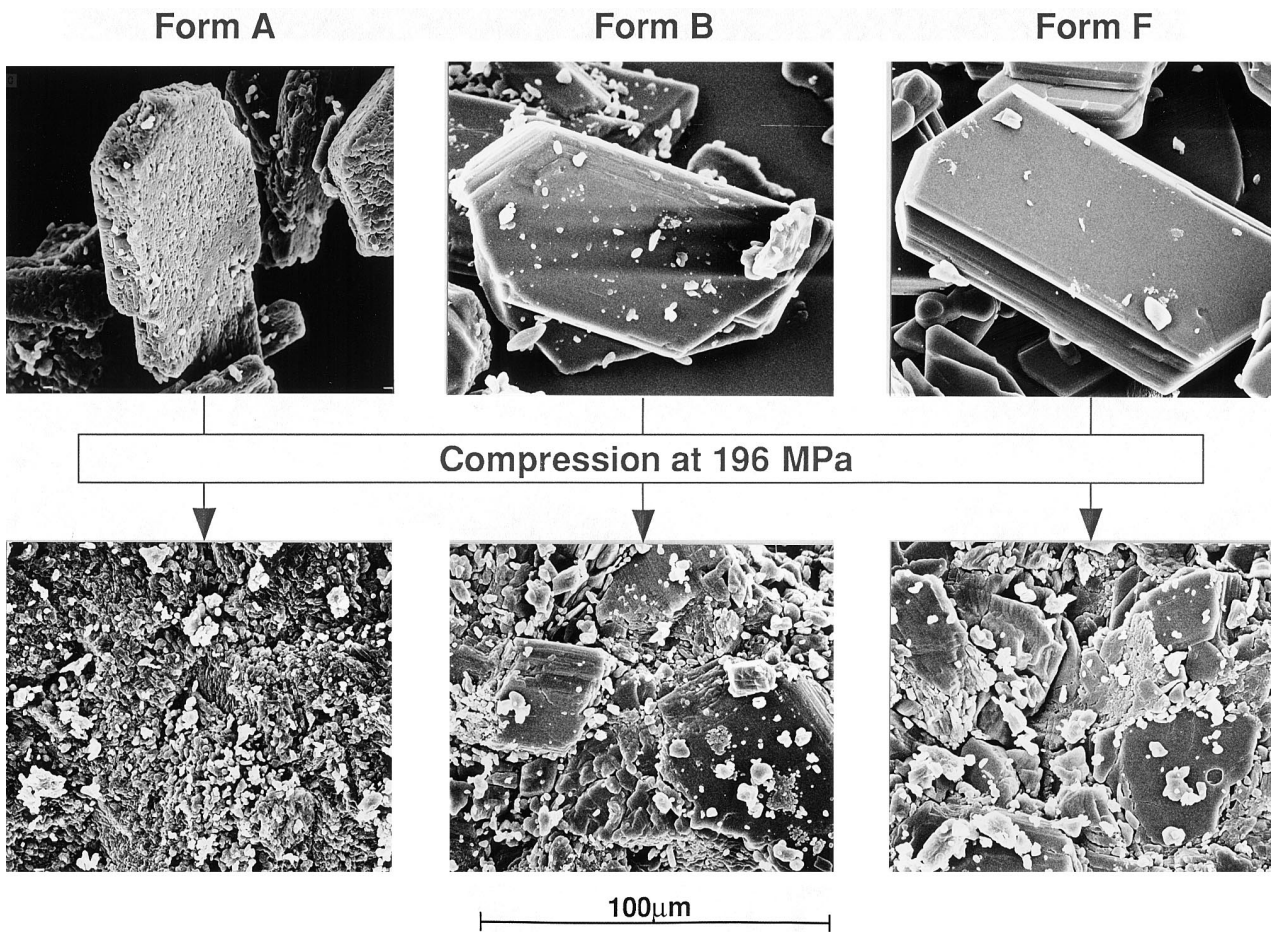


Figure 7. SEM photographs of the modifications before and after compression.

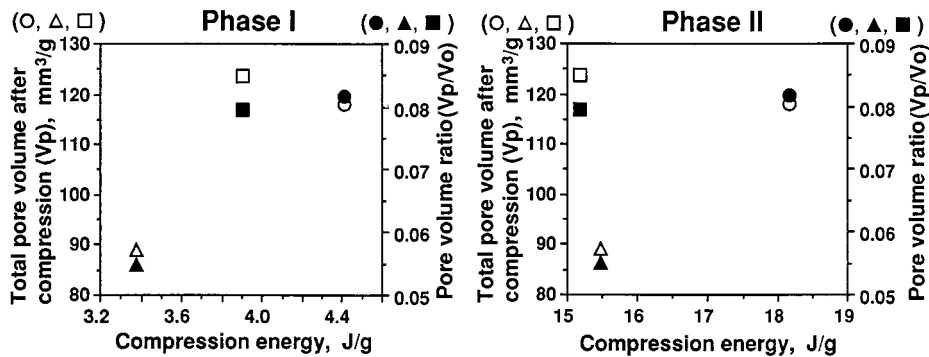


Figure 8. Relationship between the void space of tablets and/or their ratio and the compression energies of phases I and II: ○●, form A; △▲, form B; □■, form F.

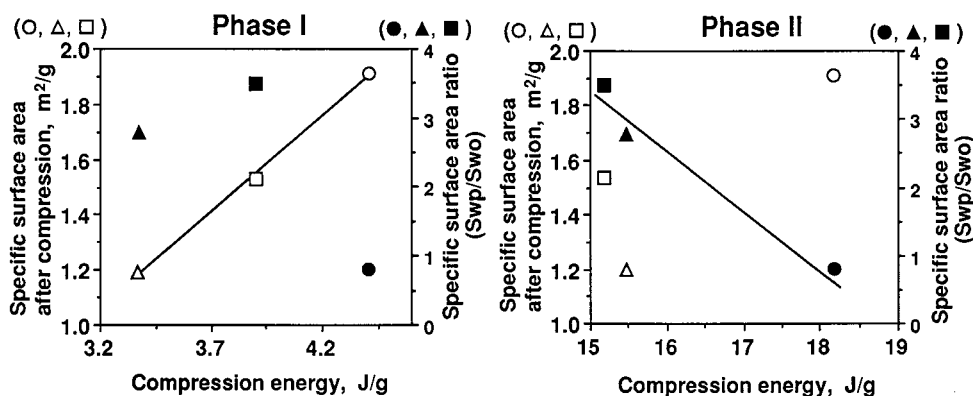


Figure 9. Relationship between specific surface area of tablets and/or their ratio and compression energies of phases I and II: ○●, form A; ▲▲, form B; □■, form F.

the ratio showed a linear relationship with compression energy at phase II, but the specific surface area did not.

Figure 10 shows the relationship between the tablet hardness and total compression energies. The tablet hardness of all forms increased with increasing compression energy, and that of form A was about three times those of forms B and F.

Figure 11 shows the relationship between the tablet hardness and the compression energies of phases I and II. The compression energies of phase II were about fivefold larger than those of phase I. The compression energies of both phases of form A were about twofold to threefold larger than those of forms B and F.

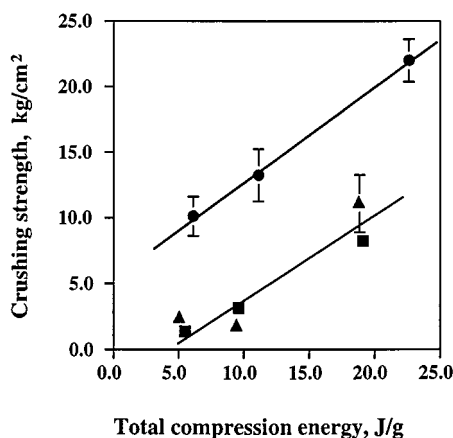


Figure 10. Relationship between the tablet hardness and the total compression energies of polymorphic forms: ●, form A; ▲, form B; ■, form F.

Figure 12 shows the relationship between the tablet hardness and the specific surface area of various polymorphic forms and/or their ratio before and after compression. The tablet hardness showed a linear relationship with the specific surface area ratio, but not with the specific surface area itself.

DISCUSSION

Effects of Polymorphic Forms of Phenobarbital Modifications on Tablet Characteristics

The specific diffraction patterns of all modifications showed no changes after compression at 196 MPa except for decreases in the diffraction intensity at a low diffraction angle ($2\theta = 7.4^\circ$ for forms B and F) due to crystal disorientation, as shown in Fig. 1. These observations suggested that the polymorphic forms were stable under our experimental conditions. Since forms A, B, and F had specific powder characteristics during dynamic tableting, the compression behavior of form B (Fig. 2) was almost the same as that of form F, but the powder bed thickness of form A was much larger than those of forms B and F.

Since the ejected tablet properties (Tables 3 and 4) reflected the powder characteristics of polymorphic forms, the order of tablet tensile strength obtained from all phenobarbital polymorphs was form A > form B > form F, in accordance with that of the specific surface area. However, the thickness and the cumulative pore volume (Fig. 6) of ejected tablets were of the order form A > form F > form B and form F > form A > form

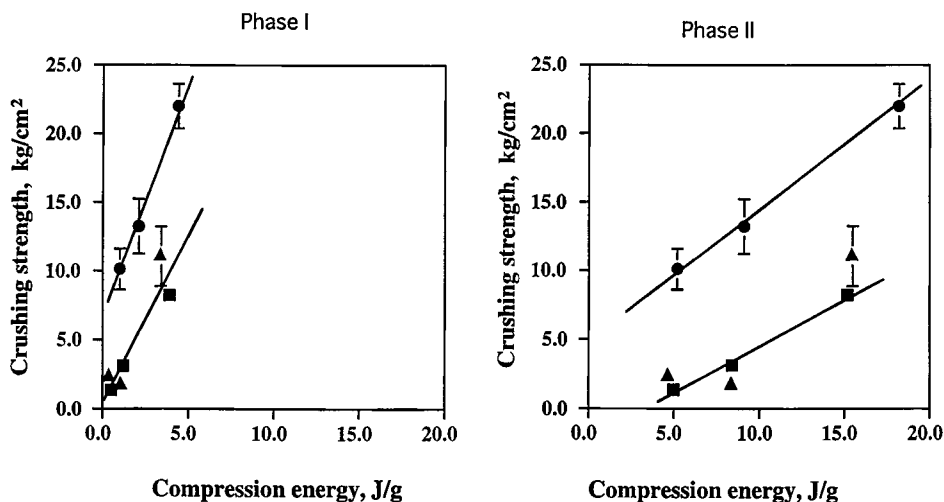


Figure 11. Relationship between the tablet hardness and the compression energies of phases I and II of polymorphic forms: ●, form A; ▲, form B; ■, form F.

B, respectively. Since the tablets of form A had large pores of about 100 μm , it may be interparticle void space between aggregated particles because form A was porous particles, including micropores with less than 2 μm pores. The tensile strength, thickness, and pore volume of tablets conflicted with each other, and therefore the tablet mechanical strength was not governed only by the particle surface area.

Since these polymorphic samples showed distinct morphological differences (Fig. 7), SEM observation before and after compression of tablets was performed. After compression at 196 MPa, form A consisted of po-

rous plate particles compressed and deformed to relatively flat surface tablets with fine micropores, but forms B and C consisted of larger single-plate particles that were compressed to irregular surface tablets with larger variations in particle size. Thus, the particles of forms B and F were broken/fragmented, giving rise to a very wide range of particle sizes during compression. This suggested that form A particles had flexible characteristics against compression stress, while forms B and F were brittle and underwent fragmentation, reflecting the crystal characteristics discussed in the previous section.

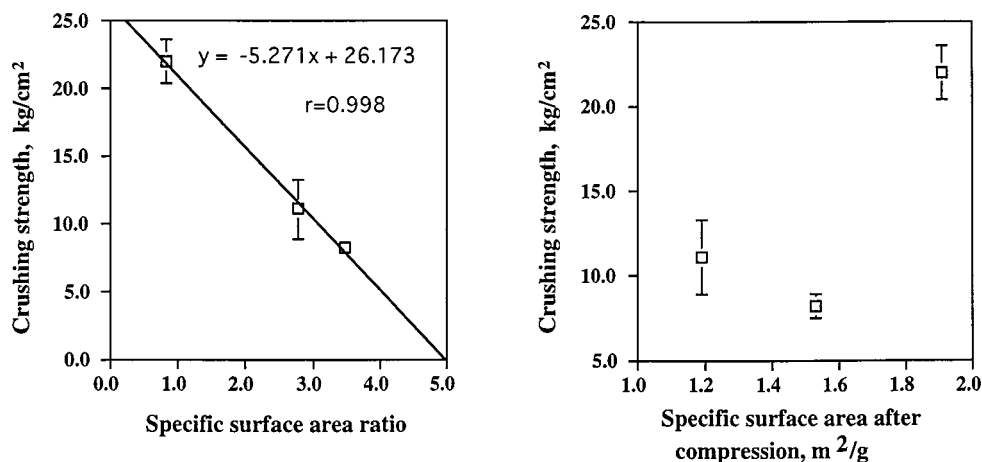


Figure 12. Relationship between the tablet hardness and the specific surface area and/or their ratio.

Effects of Polymorphic Form of Phenobarbital Modifications on the Dynamic Compression Process

To clarify the consolidation of pharmaceutical materials, we evaluated dynamic compression parameters using the Cooper and Eaton method, which is based on dividing the compression processes into two stages, particle rearrangement and fragmentation and/or deformation. Cooper and Eaton (17) reported that the compression parameters reflected the compression mechanism of powders as follows: the dimensionless coefficients a_1 and a_2 indicate the fraction of theoretical compression that would be achieved at infinite pressure by each process, and their total ($a_1 + a_2$) is unity when compression can be completely described in terms of two separate processes. When the sum ($a_1 + a_2$) is less than unity, this indicates that other processes must become activated before compression can be completely achieved. The coefficients k_1 and k_2 with units of pressure indicate the magnitude of the pressure when the particular process had the greatest probability density.

The compression parameters shown in Table 2 suggested that the compression process of form A resisted during the phase I process relative to those of forms B and F, indicating that form A had poorer powder flowability than the other forms. Therefore, the compression pressure increased at lower apparent powder volume during particle rearrangement. In contrast, the phase II compression process of form A progressed further than those of the other forms, indicating that form A was more sensitive to crystal fragmentation and/or deformation by compression pressure after filling the minimum void space in the powder bed.

The a_1 values of all forms of phenobarbital polymorphs increased with increasing compression pressure, but the a_2 values decreased. The $a_1 + a_2$ values of all compression forces increased with increasing pressure and approached 1, but the value of form A at 49 MPa (0.899) was the lowest obtained. This result suggested that both compression processes overlapped because the organic particles were soft and no fragmentation occurred. The k_1 and k_2 values of form A were larger than those of forms B and F at each compression pressure tested. Cooper and Eaton (17) reported that the k_1 and k_2 values increased with increases in material hardness, and the sum $a_1 + a_2$ of hard materials, and the value of alumina and silica were 0.850, respectively, indicating that other processes became operative before complete compression was achieved. Therefore, it seemed that the compaction behavior of form A at the lower compression

pressure of 49 MPa was more similar to that of hard material than the behavior of other forms. Particles of forms B and F were more brittle and showed a greater degree of fragmentation than those of form A, as shown in SEM photographs.

The relationship (Fig. 5) between compression energies of phases I and II and maximum compression stress indicated that form A powder required more energy at phase I than the other samples, which may have been caused by the powder flowability. Therefore, the tableting energy differences between the three polymorphic forms examined here were mainly caused by phase I, that is, the process of particle rearrangement.

On the other hand, it is well known that the compression energy at phase II reflects the physical properties of crystalline forms (17). The compression energy at phase II was almost the same as for other samples at lower pressure, except for that of form A at 196 MPa, indicating that there were no marked differences in crystal hardness among the polymorphic forms because the crystals consisted of the same molecule, phenobarbital.

Relation Between Tablet Physical Properties and Tablet Compression Parameters of Phenobarbital Polymorphic Forms

To clarify the consolidation mechanism, we investigated the relationship between tablet physical properties and tablet compression parameters. The tablet mechanical strength (Fig. 10) was dependent on the compression energy, and was affected by the polymorphic form. However, the tablet mechanical strength (Fig. 11) was affected by compression energies of both phases I and II, indicating that tablet consolidation was not significantly dependent on the input energies of both compression processes.

On the other hand, compression energies showed no linear correlations with space of tablets and/or their ratio (Fig. 8). Therefore, the void space ratio and void space were not useful parameters for estimating tablet mechanical strength.

In contrast, specific surface area after compression and compression energy at phase I showed a good linear correlation line because the powder friction increased with increases in specific surface area, but their ratio did not (Fig. 9). Therefore, it seems that the loss of energy by particle rearrangement during phase I increased with increasing specific surface area. On the other hand, the specific surface area ratio showed a linear relationship with the compression energy at phase II, but their ratio did not.

The specific surface area ratio decreased with increasing compression energy during phase II because phase II involved fragmentation and plastic flow in tableting compression; thus, the powder particles were fragmented, deformed, or broken by the compression energy. The tablet mechanical strength (Fig. 11) was dependent on the compression energies of both phases I and II.

The tablet hardness (Fig. 12) showed a linear relationship with the specific surface area ratio, but not with the specific surface area, indicating that the mechanical strength of tablets was dependent on the surface area for bonding between the particles, but not on total surface area.

ACKNOWLEDGMENT

This work was supported in part by a Grant-in-Aid for Scientific Research from the Ministry of Education, Science, and Culture, Japan.

REFERENCES

1. C. F. Lerk, A. C. Andreade, A. H. De Boer, G. K. Bolhuis, K. Zuuramn, P. De Hoog, K. Kussendrager, and J. Van Leverink, *J. Pharm. Pharmacol.*, **35**, 747–748 (1983).
2. M. Otsuka, N. Kaneniwa, K. Otsuka, K. Kawakami, O. Umezawa, and Y. Matsuda, *J. Pharm. Sci.*, **81**, 1189–1193 (1992).
3. M. Otsuka and Y. Matsuda, in *Encyclopedia of Pharmaceutical Technology*, Vol. 12 (J. Swarbrick and J. C. Boylan, eds.), Marcel Dekker, New York, 1995, pp. 305–326.
4. G. Alderborn, P. Pasanen, and C. Nyström, *Int. J. Pharm.*, **23**, 79–86 (1985).
5. J. R. Britten and N. Pilpel, *J. Pharm. Pharmacol.*, **30**, 673–677 (1978).
6. H. K. Chan and E. Doelker, *Drug Dev. Ind. Pharm.*, **11**, 315–332 (1985).
7. M. Duberg and C. Nyström, *Acta Pharm. Suec.*, **19**, 421–436 (1982).
8. M. Duberg and C. Nyström, *Powder Technol.*, **46**, 67–75 (1986).
9. J. T. Fell and J. M. Newton, *J. Pharm. Sci.*, **60**, 1866–1869 (1971).
10. J. S. Hardman and B. A. Lilley, *Nature*, **228**, 353–355 (1970).
11. J. A. Hersey, J. E. Rees, and E. T. Cole, *J. Pharm. Sci.*, **62**, 2060 (1973).
12. J. A. Hersey, G. Bayraktar, and E. Shotton, *J. Pharm. Pharmacol.*, **19**, 24s–30s (1967).
13. P. Humbert-Droz, D. Mordier, and E. Doelker, *Pharm. Acta Helv.*, **57**, 136–143 (1982).
14. G. Ibrahim, F. Pisano, and A. Bruno, *J. Pharm. Sci.*, **66**, 669–673 (1977).
15. M. Otsuka, T. Matsumoto, and N. Kaneniwa, *J. Pharm. Pharmacol.*, **41**, 665–669 (1989).
16. M. Otsuka, T. Matsumoto, S. Higuchi, K. Otsuka, and N. Kaneniwa, *J. Pharm. Sci.*, **84**, 614–618 (1995).
17. A. R. Cooper and L. E. Eaton, *J. Am. Ceram. Soc.*, **45**, 97–101 (1962).
18. R. W. Heckel, *Trans. Metall. Soc. AIME*, **221**, 671–675 (1961).
19. R. W. Heckel, *Trans. Metall. Soc. AIME*, **221**, 1001–1008 (1961).
20. T. Y. Huang, *Acta Pharm. Intern.*, **2**, 43–68 (1951).
21. B. Cleverley and P. P. Williams, *Tetrahedron*, **7**, 277–288 (1959).
22. R. J. Mesley, R. L. Clements, B. Flaherty, and K. Goodhead, *J. Pharm. Pharmacol.*, **20**, 329–340 (1968).
23. H. M. El-Banna, A. R. Ebian, and A. A. Isomail, *Pharmazie*, **30**, 455–460 (1975).
24. O. I. Corrigan, K. Sabra, and E. M. Holohan, *Drug Dev. Ind. Pharm.*, **9**, 1–20 (1983).
25. H. Nogami, T. Nagai, and T. Yotsuyanagi, *Chem. Pharm. Bull.*, **17**, 499–509 (1969).
26. K. Kato and F. Watanabe, *Yakugaku Zasshi*, **98**, 639–648 (1978).
27. M. Otsuka, M. Onoe, and Y. Matsuda, *Pharm. Res.*, **10**, 577–582 (1993).
28. S. Kopp, C. Beyer, E. Graf, F. Kubel, and E. Delker, *J. Pharm. Pharmacol.*, **41**, 79–82 (1988).
29. K. Yamaoka, T. Tanigawara, T. Nakagawa, and T. Uno, *J. Pharmacokinetics-Dyn.*, **4**, 879–885 (1981).

Copyright of Drug Development & Industrial Pharmacy is the property of Taylor & Francis Ltd and its content may not be copied or emailed to multiple sites or posted to a listserv without the copyright holder's express written permission. However, users may print, download, or email articles for individual use.